Dynamic Behavior of Cryogen Spray Cooling: Effects of Spurt Duration and Spray Distance

Guillermo Aguilar, PhD,[1,2]* Guo-Xiang Wang, PhD,[3] and J. Stuart Nelson, MD, PhD[1,2]
[1]*Department of Biomedical Engineering, University of California, Irvine, California 92697*
[2]*Beckman Laser Institute, University of California, Irvine, California 92612*
[3]*Department of Mechanical Engineering, University of Akron, Ohio 44325*

Background and Objectives: Cryogen spray cooling (CSC) is used to minimize the risk of epidermal damage during laser dermatologic surgery. Since optimization of CSC permits the safe use of higher light doses, which improves therapeutic outcome in many patients with superficial skin lesions, studies have focused on understanding spray–surface interactions and cooling dynamics. The objective of this study is to measure accurately temperature variations at the sprayed surface and the effects of spurt duration (Δt) and nozzle-to-sprayed surface distance (L) on cooling dynamics during CSC.
Study Design/Materials and Methods: A fast-response temperature measurement sensor is built using thin (20 μm) aluminum foil placed on top of a poly methylmethacrylate resin (Plexiglass®) with a 50 μm bead diameter thermocouple positioned in between. Liquid film residence time (t_r) and minimum surface temperature (T_{min}) are systematically measured as a function of Δt and L.
Results: Two distinct spray–surface interaction mechanisms are recognized. The transition between them occurs at a critical length $L_c \approx 25–30$ mm. Noticeable characteristics include: (1) for spurts at $L < L_c$, shorter t_r, and lower T_{min} are reached as compared to $L > L_c$, T_{min} is dependent on Δt and L, while t_r is a function of Δt only; (2) for spurts at $L > L_c$, T_{min} still depends on L but not on Δt, while t_r becomes a function of both Δt and L. Finally, for all Δt, t_r reaches a maximum at $L = 40$ mm.
Conclusions: Based on our results, a good choice to achieve low T_{min} and t_r for the treatment of superficial skin lesions may be met by using Δt of ≈30–50 milliseconds and the shortest spray distance that is tolerable by the patient. Spurt durations (Δt) of more than 30–50 milliseconds at spray distances (L) greater than L_c lead to higher T_{min} and longer t_r. These parameters may be appropriate for laser therapy of deeper targets. Lasers Surg. Med. 32:152–159, 2003. © 2003 Wiley-Liss, Inc.

Key words: cooling selectivity; cryogen layer; cryogen droplets; droplet momentum; surface heat flux; skin cooling

INTRODUCTION

The importance of cryogen spray cooling (CSC) during laser therapy of various dermatoses, such as port wine stains (PWS) [1,2], telangiectasias, hemangiomas [3], and rhytides [4] has been documented in a comprehensive review by Nelson et al. [5]. In short, CSC prevents excessive heating of the superficial skin layers, while minimally affecting the underlying targeted structures [1], avoiding complications such as hypertrophic scarring or dyspigmentation [6], and allowing the safe use of higher light doses.

CSC is particularly necessary for treatment of superficial vascular lesions, since it permits: (1) accurate control of the cryogen application time (typically 5–100 milliseconds) and, consequently, cooling time and; (2) high heat transfer rates as cryogen is deposited onto the skin and evaporates at the sprayed surface. These two characteristics are instrumental to achieve efficient and spatially selective epidermal cooling. To determine cooling efficiency [7] and maximal permissible light dose, the overall heat extraction (Q) or heat flow rate (q) through the skin surface must be determined. Several studies have attempted to determine these parameters and/or the heat transfer coefficient (h). In relation to CSC, this coefficient associates q to the temperature difference between the sprayed surface (T) and a meaningful average temperature of the cooling medium (T_c), for example, that of cryogen film, as given by Newton's cooling law:

$$q = hA(T - T_c),$$

where A represents the sprayed surface area. Using radiometric surface temperature measurements of human skin, Anvari et al. [8] first reported CSC-h values of 40,000 W/m^{2}K and minimum surface temperature measurements of −10°C. These measurements were valid for 5–80 milliseconds spurts using a fuel injector positioned at 20 mm from the sprayed surface. Subsequently, Torres et al. [9] used a skin phantom composed of an epoxy block with skin-like thermal properties and several 30 μm-size thermocouples embedded at depths ranging from 20 to 400 μm. The

Contract grant sponsor: National Institutes of Health; Contract grant numbers: GM 62177, HD42057; Contract grant sponsor: The Beckman Laser Institute Endowment.
*Correspondence to: Guillermo Aguilar, PhD, Beckman Laser Institute, 1002 Health Sciences Road East, Irvine, CA 92612-1475. E-mail: gaguilar@io.bli.uci.edu
Accepted 20 September 2002
Published online in Wiley InterScience (www.interscience.wiley.com).
DOI 10.1002/lsm.10133

magnitude of h was then computed through an inverse heat conduction problem (IHCP) algorithm. It was shown that for a cryogen film temperature (T_c) of -44°C, h values as low as 2,400 W/m^{2}K were required to match the measured temperatures at different depths in the epoxy. Using the same experimental approach and an analytical solution to the heat conduction equation, Verkruysse et al. [10] showed that for a similar T_c (-49°C) [11] and a wide range of h values [5,900-30,000 W/m^{2}K], it was possible to correlate equally well the temperature measurements taken 90 μm below the surface with theoretical predictions, suggesting little sensitivity of the epoxy block to large thermal variations at the surface. However, Tunnell et al. [12] showed that using a sequential function specification (SFS) method [13], it is possible to reduce the large noise associated with IHCPs and, thus, obtain more stable solutions of q and h with the same epoxy block used by Torres et al. [9].

In previous works [10,14–18], we have used basically two types of temperature sensors. The first sensor is based on a steady-state heat flux through a metal rod embedded in a thermal insulator, for example, epoxy. The rod is heated at one end with a constant temperature or heat flux source and cooled down at the other end by a continuous cryogen spurt. Using several thermocouples placed close to the cooled end at known distances from each other, the temperature gradient along the rod is measured to compute q and h [10,14].

The second sensor consists of a silver-disk detector also embedded in epoxy [19]. The upper surface of the disk is exposed to the cryogen spray and the disk temperature monitored by a small thermocouple attached to its lower surface. With such a sensor, we have quantified average values of h and q produced by nozzles of different geometries [14,15], spurt durations, spray distances [15,16], and during a series of cryogen spurts [17,18]. Although this sensor has allowed us to investigate some of the dynamic features of CSC, which are either lost with the metal rod or are not measurable with the epoxy block, it is important to recognize that the thermal inertia of the silver disk is relatively large (~100 milliseconds) and, therefore, it is not possible to resolve the "real-time" surface temperature within the range of clinically relevant spurt durations (5–100 milliseconds).

The importance of real-time surface dynamics is that fundamental information such as, temperature fluctuations, boiling, and evaporation of liquid cryogen and frost formation, among others, may be better understood. From a practical point of view, issues such as cryogen film residence time, optimal spurt duration, and spray distance, may also be more clearly established.

In the present work, we introduce a simple sensor to measure accurately "real-time" temperature variations at the sprayed surface. We use this new sensor to measure systematically the surface temperature as a function of spurt duration (Δt) and nozzle-to-sprayed surface distance (L). Finally, we compute liquid film residence time (t_r) and minimum surface temperature (T_{min}) to determine the effects of Δt and L on surface temperature dynamics.

MATERIALS AND METHODS

Cryogen Delivery and Nozzle

The cryogen utilized is 1,1,1,2 tetrafluoroethane, also known as R134a, with boiling temperature $T_b \approx -26.2^\circ$C at atmospheric pressure. Cryogen is kept in a container at saturation pressure, which is approximately 660 kPa at 25°C (95.7 psi), and delivered through a standard high-pressure hose to an electronically controlled fuel injector, to which a straight-tube nozzle is attached. This nozzle is made of stainless steel with an inner diameter (d_N) and length (l_N) of 0.7 mm (0.027 inch) and 63.6 mm (2.5 inch), respectively. The tube is soldered to a custom-made copper coupling, which in turn fits tightly around the fuel injector. The nozzle diameter is similar to that of commercial devices (e.g., DCD for SPTL-1b™ and ScleroPLUS™; $d_N \approx 0.8$ mm). Moreover, despite the fact that the cryogen container of all commercial nozzle devices is intentionally heated to raise its pressure by 15–20% above 660 kPa and, thus, avoid cryogen evaporation along the delivery lines, a previous study [11] has shown that the properties of the sprays produced by our custom-made stainless steel tube nozzles ($d_N \approx 0.7$ mm) which are attached to room temperature cryogen containers, are very similar to those of all commercial nozzles: SPTL-1b and ScleroPLUS ($d_N \approx 0.8$ mm) and GentleLASE™, Smoothbeam™, and Vbeam™ ($d_N \approx 0.5$ mm).

Temperature Measurement Sensor

Three sensors are used to measure variations in surface temperature induced by various spurt durations (Δt). The first sensor consists of a custom-made silver-disk (10.48 mm diameter, 0.42 mm thickness), embedded in an epoxy thermal insulator. The upper surface of the disk is exposed to the cryogen spray, and the disk temperature (T) is monitored by a type-K thermocouple (~300 μm bead diameter) attached to its lower surface. This sensor is designed to operate under the assumption of lumped capacitance, which means that T varies uniformly over the entire disk and that the disk *relaxation time*—given by $(\rho_m V_m c_m)/(A_m h)$, is much larger than the *diffusion time*-across its disk thickness—given by (d_m^2/α); where ρ_m, V_m, c_m, A_m, h, d_m, and α are density, disk volume, specific heat, cross sectional area, heat transfer coefficient, thickness, and thermal diffusivity, respectively. A design consideration is to keep the disk specific heat per unit volume ($\rho_m c_m$) close to that of a slab of human skin of the same diameter, which guarantees that the overall heat extracted by a given spurt duration (Δt) is approximately the same for the disk as for skin. The second sensor is identical to that described above, except that the silver-disk is smaller (3.18 mm diameter, 0.17 mm thickness).

The third sensor consists of a thin (20 μm) aluminum foil (15×10 mm) attached to a small type-K thermocouple (~50–70 μm bead diameter) on the lower surface and exposed to the cryogen spurt on the upper surface. The lower surface is positioned on top of a 12.5 mm (½ inch) square bar of poly methyl-methacrylate resin (Plexiglass). Small strips of cellulose tape (Scotch tape) of 50 μm

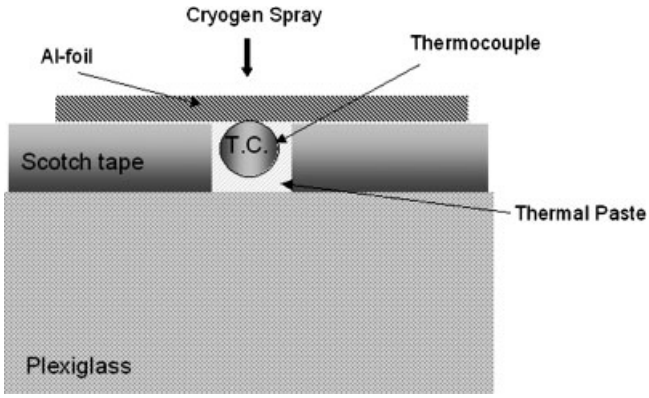

Fig. 1. Schematic of the thin Al-foil experimental sensor.

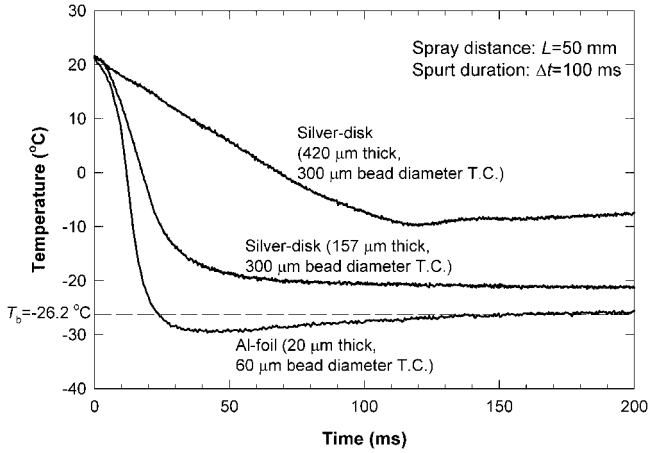

Fig. 2. Temperature measurements vs. time for the three experimental sensors. All measurements were carried out at spray distance (L) = 50 mm and spurt duration (Δt) = 100 milliseconds. Note the much shorter response time of the Al-foil sensor with the 0.001 inch (50–70 μm bead diameter) thermocouple compared to that of the metal disk detectors.

thickness are placed between the foil and substrate, forming a square box around the thermocouple bead to provide thermal insulation and mechanical support. Thermal paste is applied around the bead to ensure good thermal contact (Fig. 1). The purpose of this sensor is to provide a skin-like thermal substrate, so that Q and q through the surface are on the same order of magnitude as those expected from human skin. A small metallic foil coupled with a miniature temperature sensor provides "real-time" surface temperature measurements.

Published thermal properties of the materials used to build these sensors are shown in Table 1. Thermal properties of epidermal human skin [20] are also given for comparison. All thermocouple measurements are acquired at 4 kHz and converted to temperature data using an A/D converter board and dedicated software (InstruNet™, Omega Engineering, Stamford, CT). This acquisition rate is appropriate considering that the response time (τ) of the Al-foil attached to the thermocouple sensor is estimated to be ~3 milliseconds, where τ is defined as $\tau = hA/\rho cV$ and h, A, ρ, c, and V are the surface heat transfer coefficient (assumed to be 10,000 W/m^2 K) and sensor's surface area, density, specific heat, and volume, respectively.

RESULTS

Temperature Sensors

Figure 2 shows the temperature measurements as a function of time measured by each sensor described above. For all measurements, the nozzle-to-surface distance (L) was 50 mm, and the spurt duration (Δt) was 100 milliseconds. The response time and minimal temperature measured decrease as the thermal inertia of the sensor decreases (i.e., as the volume of the sensor plus the thermocouple decreases). This figure illustrates that the Al-foil sensor with the smallest thermocouple resolves fast temperature changes at the surface better than other sensors previously used. This capability is critical to understanding the dynamics of short spurts (5–100 milliseconds) which are used clinically. The Al-foil sensor is used for all the experiments presented below.

Preliminary Characterization

Figure 3 shows a typical surface temperature measurement by the Al-foil sensor in response to CSC. As spray droplets impinge on the surface, a rapid decrease in temperature (quantitatively similar to that expected to occur on human skin) is noted. A minimum surface temperature ($T_{\min}$) is reached at a certain time ($t_{T\min}$) which, depending on spurt duration (Δt) and/or spray distance (L), occurs at the end or shortly after spurt termination. We

TABLE 1. Thermal Properties and Thickness of Layers Used for the Al-Foil Device

Properties	Al	Scotch tape®	Delrin®	Plexiglass®	Epidermis
Thickness [mm]	0.020	0.050	25	19	—
k [W/(m K)]	205	0.19–0.25	0.36	0.19–0.24	0.21
ρ [kg/m^3]	2,710	1,160–1,400	1,410	1,150–1,190	1,200
c [J/(kg K)]	896	1,400	1,200–1,400	1,300–1,500	3,600
α_{avg} [m^2/second]	844×10^{-7}	1.22×10^{-7}	1.96×10^{-7}	1.31×10^{-7}	0.486×10^{-7}

Average epidermal skin properties also provided for reference.

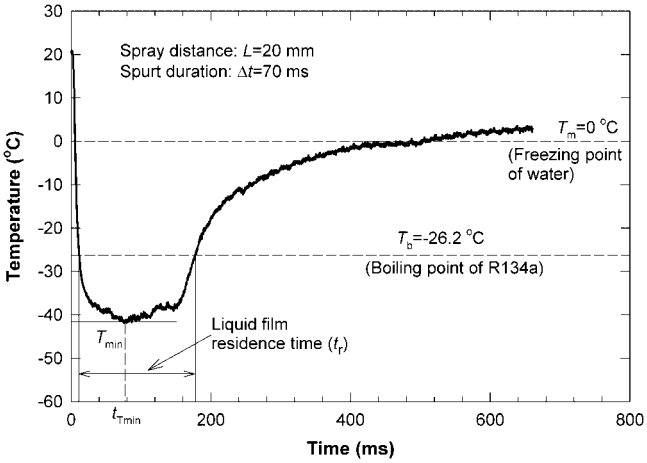

Fig. 3. Schematic of a typical temperature curve vs. time for a spurt at spray distance (L) = 20 mm from the surface and spurt duration (Δt) = 70 milliseconds. Characteristic features are minimum temperature ($T_{\min}$); time at which $T_{\min}$ is reached ($t_{T\min}$); liquid cryogen residence time (t_r); boiling point (T_b) and; freezing point (T_m).

define a liquid film residence time (t_r) as the period when the temperature is lower than the cryogen boiling point ($T_b \approx -26.2^\circ$C) at atmospheric pressure. Sometimes, a plateau is noted at the freezing temperature of water ($T_m = 0^\circ$C), which may be attributed to freezing and subsequent melting of the ambient water condensing from the atmosphere and freezing on the surface. As explained in previous works [10,11,21], water condensation and freezing on the sprayed area do not take place during the spurt despite the subzero temperatures spray droplets and the sprayed surface may reach. This is because tetrafluoroethane is a hydrophobic compound, which impedes the mixing of cryogen with water and, therefore, does not allow frost to form on the sprayed surface until the cryogen has evaporated completely. Since total evaporation takes place several milliseconds [21] to even seconds after spurt termination, only spurt duration (Δt) and residence time (t_r) are of importance for practical purposes.

Figure 4a shows temperature as a function of time for spurt durations (Δt) of 10, 20, 30, 40, and 50 milliseconds, where spray distance (L) is kept constant at 50 mm. Figure 4b shows similar results for Δt of 60, 80, 100, 120, and 150 milliseconds. For this spray distance, minimum surface temperature ($T_{\min}$) and the time it takes to reach it ($t_{T\min}$) are $\approx -30^\circ$C and 40–50 milliseconds, respectively, and are nearly identical for all Δt. It should also be noted that for $\Delta t < 50$ milliseconds, the increase in temperature from $T_{\min}$ to T_b is very gradual and relatively linear, while for $\Delta t > 60$ milliseconds, an oscillatory pattern around T_b can be distinguished. This pattern may be attributed to the presence of a residual cryogen layer, which undergoes a very dynamic boiling process after spurt termination, and it is more noticeable for longer spurts.

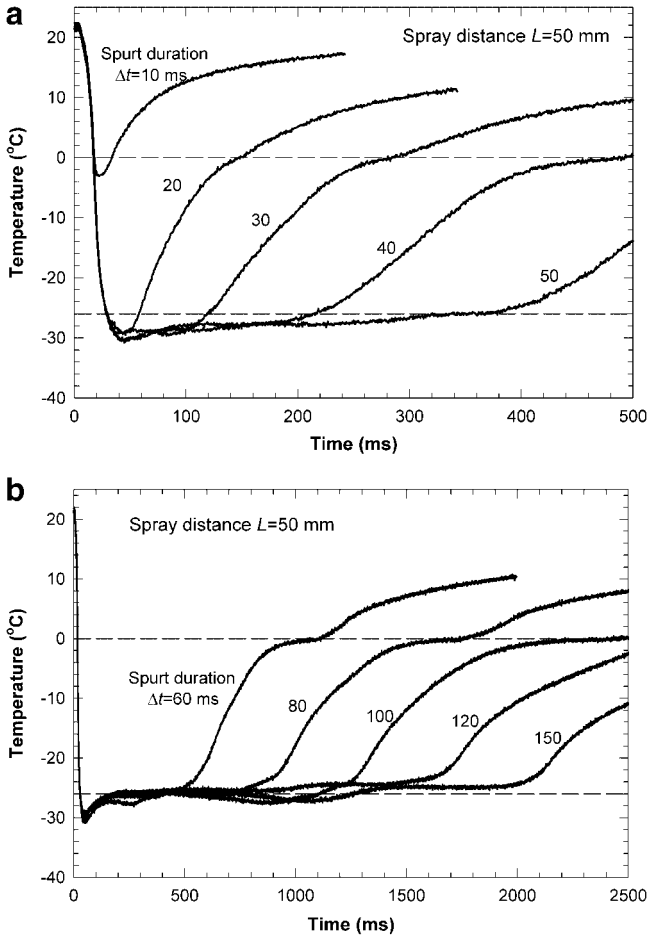

Fig. 4. **a**: Temperature vs. time for spurt durations $\Delta t = 10$–50 milliseconds and constant spray distance (L) = 50 mm. A constant minimum surface temperature ($T_{\min}$) $\approx -30^\circ$C, slightly below T_b is reached for spurts 20 milliseconds and longer, and $t_{T\min} \approx 40$–50 milliseconds is also constant for all spurts. **b**: Temperature vs. time for spurt durations $\Delta t = 60$–150 milliseconds and constant $L = 50$ mm. A constant $T_{\min} \approx -30^\circ$C and $t_{T\min} \approx 40$–50 milliseconds are reached for all spurt durations. Note the oscillatory behavior of T around T_b for all spurt durations.

Figure 5 shows temperature as a function of time at constant spray distance (L) = 25 mm for spurt durations (Δt) ranging from 10 to 60 milliseconds. The relatively constant values of $T_{\min}$ and $t_{T\min}$ with Δt seen for $L = 50$ mm (Fig. 4a–b) are not reproducible at this L. For $L = 25$ mm, $T_{\min}$ diminishes and $t_{T\min}$ increases with Δt. Note that the temperature increase after $T_{\min}$ is followed by a fall and then a gradual increase back to room temperature.

Parametric Measurements of Liquid Film Residence Time and Minimum Surface Temperature

Having distinguished the two different patterns at spray distances (L) = 25 and 50 mm, we conducted systematic

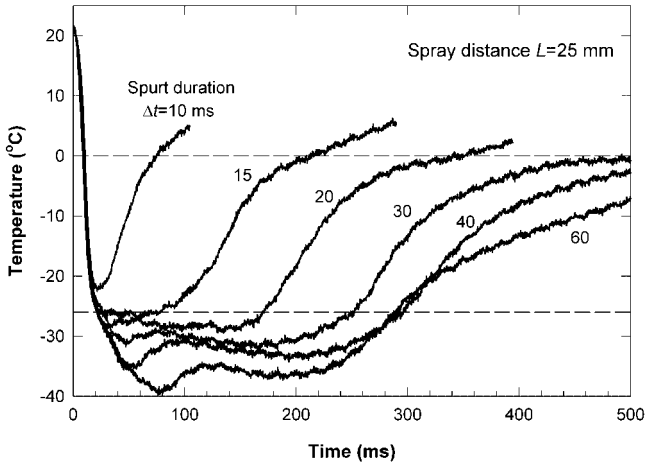

Fig. 5. Temperature vs. time for spurt durations $\Delta t = 10$–60 milliseconds and constant spray distance (L) = 25 mm. Minimum surface temperature ($T_{\min}$) and the time at which it is measured ($t_{T\min}$) are no longer invariant, as for spurts at $L = 50$ mm, but depend on Δt. Also, a secondary cooling after $t_{T\min}$ is appreciable. This is perhaps related to a more efficient boiling as the surface cryogen layer thins due to evaporation.

measurements to determine residence time (t_r) and minimum surface temperature ($T_{\min}$) by varying the two parameters of interest of this study: spurt duration (Δt) and spray distance (L). Figure 6a shows t_r as a function of Δt for various L. Spurts at $L < 25$ mm show a similar trend of overall shorter t_r, while spurts at $L > 25$ mm show a significantly longer t_r. Apparently, the critical length (L_c) where this transition takes place is ≈25–30 mm. Also note that the separation of these two patterns occurs at Δt between 10 and 20 milliseconds. For Δt shorter than 10 milliseconds $t_r = 0$, since the surface temperature never reaches −26.2°C.

Figure 6b shows residence time (t_r) as a function of spurt duration (Δt), but for spray distances (L) ≥ 40 mm. From Figure 6a,b it is evident that maximum values t_r are reached at $L = 40$ mm and then gradually decrease for $L > 40$ mm. These results suggest that spurts delivered at $L = 40$ mm deposit the maximum amount of cryogen on the surface, regardless of Δt.

Figure 7 shows residence time (t_r) as a function of spray distance (L) for various values of spurt duration (Δt). A family of curves with similar trends is appreciable. A sudden increase in t_r takes place for all curves at $L \approx 25$–30 mm, consistent with the critical spray distance (L_c) noted in Figure 6a. Note that the maximum t_r appears at longer values of L as Δt increases. This variation of t_r is actually quite large, increasing from 200 to 1,500 milliseconds for Δt of 20 and 100 milliseconds, respectively.

Finally, Figure 8a and b show variations of minimum surface temperature ($T_{\min}$) as a function of spurt duration (Δt) and spray distance (L), respectively. The presence of L_c can be seen once again in Figure 8a by the dramatic change in the trend between the measurements carried out at

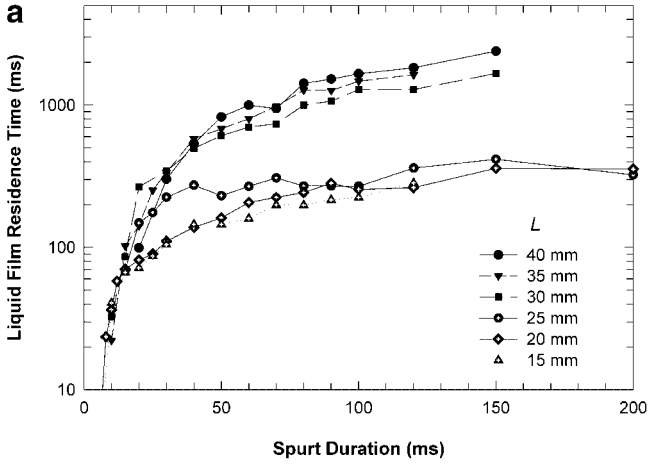

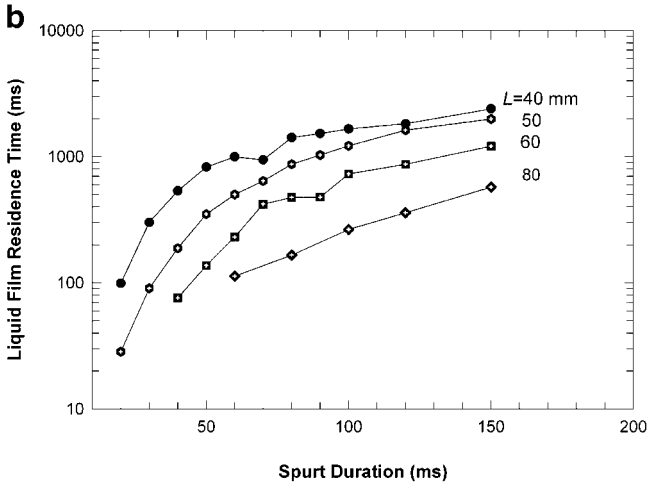

Fig. 6. **a**: Liquid residence time (t_r) vs. spurt duration (Δt) for spurts delivered at various distances from the nozzle ($L <$ 40 mm). Note the two distinct group of curves for spurts at $L < L_c$ and for those at $L > L_c$. **b**: Liquid residence time (t_r) vs. spurt duration (Δt) for spurts delivered at various distances from the nozzle ($L \geq 40$ mm). $L = 40$ mm is the spray distance where t_r reaches a maximum value, regardless of Δt.

$L = 15$ and 20 mm, as compared to those at $L = 30$ mm, and in Figure 8b by the merger at L_c of the series of curves pertaining to different Δt. It is noted that for $L < L_c$, temperatures lower than −40°C may still be reached for Δt longer than 20 milliseconds, and an asymptotic $T_{\min}$ of ≈−42°C is measured for spurt 70 milliseconds or longer. In contrast, it appears that for a given L longer than L_c, $T_{\min}$ varies similarly for all spurt durations.

By way of comparison, the curve in Figure 8b with solid circles represents the average cryogen spray temperature measured by a 300 μm type-K thermocouple inserted into the center of the spray cone [11]. Note that for spray distances (L) > 40 mm, the average spray temperature may be significantly lower than the surface temperature

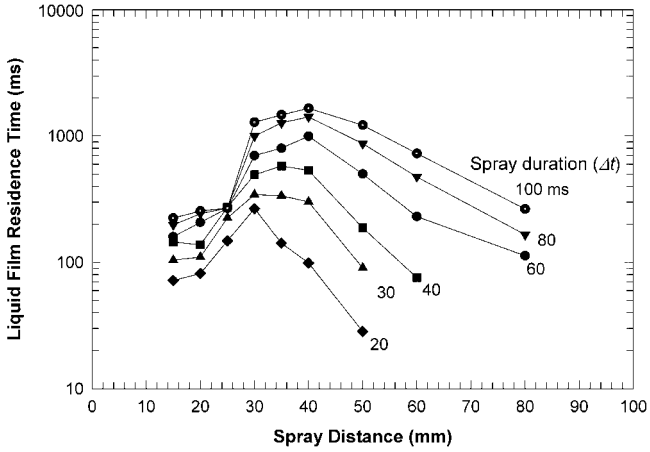

Fig. 7. Liquid residence time (t_r) vs. spray distance (L) for various spurt durations (Δt). Except for the short spurt of 20 milliseconds, all spurts show a similar $t_r \approx 250$ milliseconds at $L = 25$ mm (transition region).

($\sim$24°C) due to the continuous droplet evaporation and decreasing partial pressure of cryogen vapor as droplets travel from the nozzle to the targeted surface [22].

DISCUSSION

For this study, the choice of the thin Al-foil with the 50–70 μm bead diameter thermocouple is advantageous over the other sensors [9,10,14,19] because of its faster response time ($\tau \approx 3$ milliseconds), which is short enough to observe most of the dynamic features associated with CSC. Furthermore, as opposed to the metallic disk or rod, where the larger thermal inertia and thermal conductivity of metals could lead to somewhat large heat fluxes across the surface, the substrate of this sensor has thermal properties very close to those of human skin (see Table 1) and, thus, cooling dynamics at the surface are unlikely to depart much from the real scenario of human skin cooling.

The distinct features in the temperature measurements carried out for spray distance (L) = 50 mm (Fig. 4a,b) and 25 mm (Fig. 5), indicate a large difference in the surface dynamics. In the former case, minimum surface temperature (T_{min}) and the time at which it is measured (t_{Tmin}) are constant. In contrast, moving the nozzle closer to the surface at $L = 25$ mm shows that T_{min} decreases and t_{Tmin} increases with spurt duration (Δt). Within this range of spray distances (L), more cryogen is deposited onto the surface as Δt increases and, therefore, a longer time is needed for all cryogen to evaporate. For $L = 50$ mm, the cryogen layer evaporation occurs at a constant temperature near T_b, as evidenced by the nearly constant temperature measured before the subsequent increase. However, for $L = 25$ mm, this process appears to take place below T_b.

It seems reasonable to correlate sprays delivered at $L < L_c$ with large momentum droplets, which have not adequately dispersed at such distances and, therefore, induce a

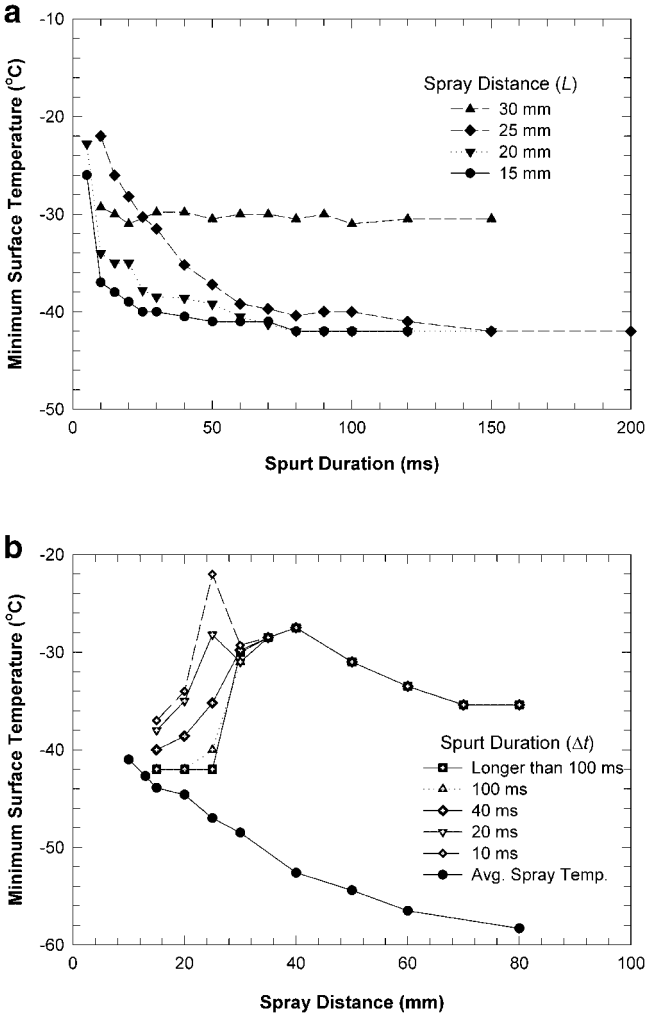

Fig. 8. **a**: Minimum surface temperature (T_{min}) vs. spurt duration (Δt) for spurts delivered at various distances from the nozzle (L). T_{min} depends on L and Δt, particularly for spurts shorter than 50–60 milliseconds, whereas T_{min} slightly varies for spurts delivered at $L = 30$ mm. **b**: Minimum surface temperature (T_{min}) vs. spray distance (L) for various spurt durations (Δt). The dependence of T_{min} on Δt for spurts at $L < 25$ mm and the invariance of T_{min} with Δt for spurts at $L > 25$ mm are noticeable.

jet-like impact onto the sprayed surface. Larger momentum sprays may either induce a large number of droplets to bounce off of the surface, or a faster lateral spreading of the cryogen layer, or both. As a result, the cryogen layer at the center of the sprayed area is likely to be thinner and would explain why residence time (t_r) is shorter for all spurt durations (Δt) at spray distances (L) $< L_c$ compared to those at $L > L_c$. Indeed, a thinner layer would also allow colder incoming droplets to reach the surface more readily, inducing lower minimum surface temperature (T_{min}) as seen in Figure 8. Note, however, that the secondary decrease in temperature following T_{min} (Fig. 5) can be also explained by the presence of a thin cryogen layer at the surface. Upon

spurt termination, the intense convective and evaporative action of many cryogen droplets impinging on the surface ceases, which is why the surface temperature starts to increase shortly after the end of the spurt. However, as the residual cryogen forming a thin layer evaporates, the boiling and convective dynamics of liquid cryogen become more efficient and further heat extraction is achieved, explaining the secondary decrease in temperature. We hypothesize that even the thickest layer formed by spurts delivered at spray distances (L) $< L_c$ is thinner than that of spurts delivered at $L > L_c$, which is why spurts delivered at $L < L_c$ show a shorter residence time (t_r) for any given spurt duration (Δt), as seen in Figure 6a.

Similar dynamic features may also be observed from the work of Torres et al. [9,23], where a thermocouple placed on the surface of the epoxy block showed that the minimal surface temperature might last as long as 680 milliseconds after a 100 milliseconds spurt. This approach, however, may have a few drawbacks for the accurate assessment of the surface temperature. First, the thermocouple bead diameter is of the same order of magnitude as the estimated cryogen film layer [14], so the disturbance to the dynamics of boiling cryogen is likely to be large. If the thermocouple bead were fully covered by the cryogen layer, it would measure the average temperature of the cryogen layer, in which a large temperature gradient may exist. Alternatively, if the cryogen layer were smaller than the dimension of the thermocouple bead, the measured temperature would reflect an average between the surface, cryogen layer, and the mixture of cryogen vapor and air surrounding the thermocouple bead.

For spray distances (L) slightly longer than L_c, the droplets become abruptly better dispersed, and residence time (t_r) increases dramatically. The overall cryogen mass deposition exceeds the droplet rebound and liquid spreading induced by droplet impact. This condition prevails until L is long enough that the increased evaporation of droplets in-flight decreases mass deposition, balancing the cryogen droplet rebound, lateral spreading of the cryogen layer, and surface layer evaporation, which is why a maximum in t_r is reached at $L = 40$ mm (Fig. 6b). Also, since $L = 40$ mm appears to produce the thickest possible layer, it is to be expected that the minimum surface temperature (T_{min}) is highest. Indeed, Figure 8b shows that T_{min} for $L = 40$ mm is the highest for all spurt durations (Δt). Finally, as L becomes longer, t_r decreases as a result of more in-flight evaporation and less droplets reaching the surface.

For laser treatment of superficial skin lesions, fast and efficient heat extraction is required to induce a large temperature difference between the target and the epidermal–dermal junction [24], which in turn provides sufficient epidermal protection during laser irradiation with minimal pre-cooling of the target. Therefore, spurts at spray distances (L) $< L_c$ and spurt durations (Δt) of 30–50 milliseconds may be the most desirable, since these parameters lead to lower minimum surface temperature (T_{min}) and shorter residence time (t_r). A lower T_{min} induces a larger temperature gradient within the skin and, therefore, a higher heat flux through the surface. A shorter t_r is an indication of lesser cryogen deposition and conceivably a thinner cryogen layer. The thinner the cryogen layer, the less likely laser light transmission may be significantly reduced during subsequent irradiation especially if and when procedures using intermittent-multiple cryogen spurts and laser pulses [7] are implemented. Unfortunately, spurts too close to the skin surface may cause patient discomfort due to the strong impact of the cryogen on human skin, as verified by the authors and a few other volunteers at the Beckman Laser Institute for this and a previous study [15].

In contrast, spray distances too far from the skin surface do not seem appropriate for the treatment of superficial skin lesions (e.g., PWS), because minimum surface temperature (T_{min}) does not reach its lowest value ($\sim 42^{\circ}$C) and residence time (t_r) exceeds 100 milliseconds for spurt durations (Δt) ≥ 30 milliseconds. At first, these statement seems to contradict the recommendations of optimal Δt between 100 and 200 milliseconds previously reported based on a numerical modeling study [24]. However, as shown here, $\Delta t = 30$ milliseconds leads to $t_r \sim 100$ milliseconds. The latter time is equivalent to the Δt used in the previous numerical study, where there was no delay between spurt termination and the laser pulse and a constant cryogen layer temperature and heat transfer coefficient (h) values were assumed.

For treatment of deeper targets, spurts at spray distances (L) $> L_c$ and spurt durations (Δt) > 30–50 may be appropriate to provide sufficient epidermal protection without cryo-injury. The reason being that less efficient cooling and longer cooling times (including a delay period after spurt termination until cryogen evaporates completely) can be used to cool the epidermal–dermal junction sufficiently prior to laser irradiation, without significantly affecting the temperature of the deeper targets.

CONCLUSIONS

A new thin-film temperature sensor was built and used to measure the dynamic cooling effects during CSC. It was shown that two distinct spray–surface dynamics occur depending primarily on spraying distance (L). In general, when sprays are $L < 25$–30 mm, shorter residence times (t_r), and lower minimum surface temperatures (T_{min}) are reached compared to those obtained when $L > 25$–30 mm. At $L = 25$–30 mm, there appears to be a critical length (L_c), where a distinct transition in the spray surface interaction takes place. This transition may be associated with sprays that have jet-like characteristics when $L < L_c$, while better-dispersed sprays are likely to prevail for $L > L_c$.

For spurts at $L < L_c$, T_{min} still decreases with increasing spurt duration (Δt). Adjusting L and Δt to obtain the lowest possible T_{min} may be a desirable condition to enhance the efficiency of heat extraction during the treatment of superficial skin lesions (e.g., PWS). However, the forceful impact of these sprays on skin when $L < L_c$ may cause patient discomfort. For all Δt, it was seen that T_{min} and t_r reach a maximum at $L = 40$ mm, which suggests that the difference between the incoming cryogen mass and the cryogen mass

loss due to droplet rebound, liquid lateral spreading, and evaporating cryogen, is minimal at this spray distance.

Spray distances (L) > L_c and spurt durations (Δt) > 30–50 milliseconds induce higher T_{min} and may increase t_r substantially. These parameters may be acceptable for the treatment of deeper targets (e.g., hair follicles), where less efficient cooling and longer cooling times are permissible.

ACKNOWLEDGMENTS

This work was supported by the National Institutes of Health (GM 62177 to JSN and HD42057 to GA). Institutional support from the Beckman Laser Institute Endowment is also acknowledged. Laboratory assistance and data analysis provided by Emil Karapetian, Odette Ma, and Misha Heller, and helpful discussions with Prof. Sol Kimel are greatly appreciated.

REFERENCES

1. Nelson JS, Milner TE, Anvari B, Tanenbaum BS, Kimel S, Svaasand LO, Jacques SL. Dynamic epidermal cooling during pulsed laser treatment of port-wine stain. Arch Dermatol 1995;131:695–700.
2. Waldorf HA, Alster TS, McMillan K, Kauvar AN, Geronemus RG, Nelson JS. Effect of dynamic cooling on 585-nm pulsed dye laser treatment of port-wine stain birthmarks. Dermatol Surg 1997;23:657–662.
3. Chang CJ, Anvari B, Nelson JS. Cryogen spray cooling for spatially selective photocoagulation of hemangiomas: A new methodology with preliminary clinical reports. Plast Reconstr Surg 1998;102:459–463.
4. Kelly KM, Nelson JS, Lask GP, Geronemus RG, Bernstein LJ. Cryogen spray cooling in combination with non-ablative laser treatment of facial rhytides. Arch Dermatol 1999; 135:691–694.
5. Nelson JS, Majaron B, Kelly KM. Active skin cooling in conjunction with laser dermatologic surgery: Methodology and clinical results. Semin Cutan Med Surg 2000;19:253–266.
6. Chang CJ, Nelson JS. Cryogen spray cooling and higher fluence pulsed dye laser treatment improve port-wine stain clearance while minimizing epidermal damage. Dermatol Surg 1999;25:767–772.
7. Aguilar G, Diaz SH, Lavernia EJ, Nelson JS. Cryogen spray cooling efficiency: Improvement of port wine stain laser therapy through multiple-intermittent cryogen spurts and laser pulses. Lasers Surg Med 2002;31:27–35.
8. Anvari B, Milner TE, Tanenbaum BS, Kimel S, Svaasand LO, Nelson JS. Selective cooling of biological tissues: Application for thermally mediated therapeutic procedures. Phys Med Biol 1995;40:241–252.
9. Torres JH, Nelson JS, Tanenbaum BS, Milner TE, Goodman DM, Anvari B. Estimation of internal skin temperature measurements in response to cryogen spray cooling: Implications for laser therapy of port wine stains. IEEE J Special Topics Quant Elect 1999;5:1058–1066.
10. Verkruysse W, Majaron B, Aguilar G, Svaasand LO, Nelson JS. Dynamics of cryogen deposition relative to heat extraction rate during cryogen spray cooling. Proc SPIE 2000;3907: 37–48.
11. Aguilar G, Majaron B, Verkruysse W, Nelson JS, Lavernia EJ. Characterization of cryogenic spray nozzles with application to skin cooling. In: Proceedings of the International Mechanical Engineering Congress and Exposition (IMECE) 2000; FED-V.253:189–197.
12. Tunnell JW, Torres JH, Anvari B. Methodology for estimation of time-dependent surface heat flux due to cryogen spray cooling. Ann Biomed Eng 2002;30:19–33.
13. Beck JV, Blackwell B, St. Clair CR, Jr. In: Inverse heat conduction: Ill-posed problems. New York, NY: Wiley; 1985.
14. Aguilar G, Verkruysse W, Majaron B, Svaasand LO, Lavernia EJ, Nelson JS. Measurement of heat flux and heat transfer coefficient during continuous cryogen spray cooling for laser dermatologic surgery. IEEE J Sel Top Quantum Electr 2001;7:1013–1021.
15. Aguilar G, Majaron B, Pope K, Svaasand LO, Lavernia EJ, Nelson JS. Influence of nozzle-to-skin distance in cryogen spray cooling for dermatologic laser surgery. Lasers Surg Med 2001;28:113–120.
16. Aguilar G, Majaron B, Viator JA, Basinger B, Karapetian E, Svaasand LO, Lavernia EJ, Nelson JS. Influence of spraying distance and post-cooling on cryogen spray cooling for dermatologic laser surgery. In: Proc SPIE 2001;4244:82–92.
17. Majaron B, Aguilar G, Basinger B, Randeberg LL, Svaasand LO, Lavernia EJ, Nelson JS. Sequential cryogen spraying for heat flux control at the skin surface. In: Proc SPIE 2001;4244: 74–81.
18. Majaron B, Svaasand LO, Aguilar G, Nelson JS. Intermittent cryogen spray cooling for optimal heat extraction during dermatologic laser treatment. Phys Med Biol 2002;47:3275–3288.
19. Svaasand LO, Randeberg LL, Aguilar G, Majaron B, Kimel S, Lavernia EJ, Nelson JS. Cooling efficiency of cryogen spray during laser therapy of skin. Lasers Surg Med 2003;32:137–142.
20. Duck FA. Thermal properties of tissue. In: Physical properties of tissue. London: Academic press; 1990.
21. Majaron B, Kimel S, Verkruysse W, Aguilar G, Pope K, Svaasand LO, Lavernia EJ, Nelson JS. Cryogen spray cooling in laser dermatology: Effects of ambient humidity and frost formation. Lasers Surg Med 2001;28:469–476.
22. Aguilar G, Majaron B, Verkruysse W, Zhou Y, Nelson JS, Lavernia EJ. Theoretical and experimental analysis of droplet diameter, temperature, and evaporation rate evolution in cryogenic sprays. Int J Heat Mass Transf 2001;44:3201–3211.
23. Torres JH, Tunnell JW, Pikkula B, Anvari B. An analysis of heat removal during cryogen spray cooling and effects of simultaneous airflow application. Lasers Surg Med 2001;28: 477–486.
24. Verkruysse W, Majaron B, Tanenbaum BS, Nelson JS. Optimal cryogen spray cooling parameters for pulsed laser treatment of port wine stains. Lasers Surg Med 2000;27:165–170.